

Numerical simulation utilizing modified fractional Euler formula for the Ebola virus model and blood ethanol concentration system

M. M. Khader ^{a*}, A. M. Shloof ^b and Halema Ali Hamead ^c

a. Department of Mathematics and Statistics, College of Science, Imam Mohammad Ibn Saud Islamic University (IMSIU), Riyadh, Saudi Arabia

b. Department of Mathematics, Faculty of Science, University of Zintan, AlZintan, Libya

c. Department of Mathematics, Faculty of Education, University of Aljufra, Aljufra, Libya

Emails: mmkhader@imamu.edu.sa^(a), aml.shloof@uoz.edu.ly^(b), halemaali20@yahoo.com^(c)

Abstract

In this study, we numerically investigate two significant medical models, Ebola Viral Disease (EVD) and Blood Ethanol Concentration (BEC) models-both formulated using Caputo-fractional derivatives. We develop and apply the Modified Fractional Euler Method (MFEM) for their solution, with a specific focus on error analysis. Comparative studies with the classical Runge-Kutta fourth-order method (RK4M) demonstrate that MFEM provides a computationally efficient and accurate alternative for solving such systems. The major features of the given procedure are its ease of application to this type of problem and other systems in various fields, in addition to the absence of numerical errors accumulating. Finally, we can control the increase in the convergence rate and the stability of the simulation process. The convergence examination and error estimation for the suggested scheme are also included. The importance of this study also lies in its contribution to our understanding of the dynamics of these two models in their fractional form. In addition, those numerical investigations demonstrate how control parameters affect specific components within these models.

Keywords: Ebola virus model; BEC system; Caputo fractional derivatives; MFEM; RK4M.

1. Introduction

The Ebola virus was named after the first known cases of Ebola in the Congo, adjacent to the Ebola River, in 1976. While uncommon, it is exceedingly fatal [1]. Research shows it intermittently affects monkeys and humans, with outbreaks reported in several other African nations. Nevertheless, numerous biologists have encountered challenges in ascertaining the origin of this virus [2]. However, many unique studies and investigations have established that mammals like bats are the primary source of EVD. This virus can infect people in several ways, such as through direct contact with human or animal tissue or the bodily fluids of a sick or deceased person [3]. In [4], a conformable derivative is used to introduce a modified mathematical model of the EVD, incorporating effective control strategies such as quarantine, self-isolation, and hospitalization. These compartments introduced a key position to understand the transmission of EVD in society. Also, the basic reproduction number (BRN); R_0 has been determined using the next-generation matrix method (NGMM) to understand the

impact of parameter variations on EVD [5,6]. Stability analysis has been calculated to assess the behavior of the virus. These findings enhance our understanding of Ebola dynamics and offer critical implications for effective outbreak control strategies. In [7], the researchers developed the EVD model to include eight components to help more deeply understand and track its dynamic transmission, and they also presented studies on the existence and uniqueness of the solution. They investigated the effects of the piecewise Caputo fractional derivatives on the model's behavior. Also, R_0 is computed for it with sensitivity analysis with various parameters effective on the spread of illness. They established the local stability and global stability with the help of the next Matignon method and the Lyapunov criterion, respectively for a feasible solution to the proposed model. The numerical solution is derived by utilizing the Newton's polynomial technique [8]. In [9], to improve the transmission dynamics of this virus by applying the intelligent model of feed-forward neural networks, a modern methodology of hybrid genetic algorithm using sequential quadratic programming (HGASQP) was proposed. This was done by defining the mean squared error as the fitness objective function to optimize HGASQP. In [10], the same model was studied more closely using the Atangana-Baleanu Caputo (ABC) fractional derivative with the Mittag-Leffler kernel. The existence and uniqueness of the solutions were proven with the help of the Picard-Lindelof approach, and two-step Lagrange polynomial interpolation was used to obtain its numerical solutions. In [11], this model was modified by adding a highly significant and physically significant term: the probability of an infected individual being born and transmitted to the current population. The proposed problem was validated using a well-known theory, and the cases of disease extinction or persistence were discussed in detail. For more information, see ([12]-[16]).

Studying chemical kinetics helps us understand and comprehend the nature of many biological changes in our daily lives. Among these changes is the development of new substances from existing reactants through chemical reactions, which can lead to the rapid spoilage of our food, the speed at which a particular tablet works, the rate of oxidation of carbon steel materials, and other changes. Some factors that affect reaction rates are the nature of the reactants, the ambient temperature, and the catalysts. Given the importance of this type of reaction, many researchers have conducted further studies and provided research data to determine reaction rates. This, in turn, has helped them derive rate laws and chemical kinetic rate constants, such as determining the reaction rate and how the reaction rate depends on the concentration of the chemicals used. It is worth noting that in recent years, interest has increased in presenting an experimental study in [17] to determine the concentration of alcohol in human blood after representing and modeling this model with a system of ordinary differential equations. These studies were then further investigated in this study to examine the same model but in fractional form [18]. In [19], a nonlinear fractional (ABC) alcohol concentration model (ACM) was developed to reflect the complex dynamics of alcohol consumption and was solved numerically using the finite difference method. Paper [20] investigated the dynamics of the ACM and the impact of addiction treatment using the continuous mathematical model in its fractional form (ABC). This significant study offers a novel approach to studying the existence & uniqueness of solutions. The author employed the NGMM to explore disease-free and endemic equilibria and calculate R_0 . In addition, they conducted the sensitivity

analysis to identify parameters that significantly influence R_0 , which helps us understand the dynamics of alcohol use and the effectiveness of intervention strategies. The local/global stability of both the alcohol-free and alcohol-present equilibria are rigorously examined to provide insights into potential long-term outcomes of alcohol consumption in the presence of treatment facilities. Furthermore, they utilized the Lagrange interpolation polynomial as a numerical framework implemented to solve the system.

2. Basic concepts of fractional calculus

Power-law memory kernels have been utilized in fractional derivative (FD) systems to modify the fractional derivatives. This makes it easier for the model to describe memory and global association. This is the paramount definition employed in the formulation of fractional calculus theory. Formulating Caputo's definition when modeling specific real-world problems addressed some of the shortcomings of the Riemann-Liouville (RL) formulation [21]. This section will present several principles of fractional calculus ([22]-[24]).

Definition 1. The RL integral of fractional order $0 < \nu < 1$ for the function $\Omega(\xi)$ is realized as [21]:

$$I^\nu \Omega(\xi) = \frac{1}{\Gamma(\nu)} \int_0^\xi (\xi - p)^{\nu-1} \Omega(p) dp. \quad (1)$$

Definition 2. The Caputo FD, D^ν of order $m-1 < \nu \leq m$, $m \in \mathbb{Z}^+$ for the function $\Omega(\xi)$ is formulated by [21]:

$$D^\nu \Omega(\xi) = \frac{1}{\Gamma(m-\nu)} \int_0^\xi (\xi - p)^{m-\nu-1} \Omega^{(m)}(p) dp. \quad (2)$$

Fractional derivatives are related to fractional integration through the following significant relationship:

$$I^\nu D^\nu \Omega(\xi) = \Omega(\xi) - \sum_{\ell=1}^m \Omega^{(\ell)}(0^+) \frac{\xi^\ell}{\ell!}, \quad \xi > 0, \quad m-1 < \nu \leq m. \quad (3)$$

3. Description the proposed problems

3.1. Formulation the BEC system

This study will utilize the primary source to acquire authentic data through the experiments given in [25] to formulate the mathematical equations that classify the model under surrogate, which ascertains the concentration of alcohol in the human stomach $\theta_1(t)$ & in the bloodstream $\theta_2(t)$ at any given time t .

The proposed model is represented as a system of fractional differential equations (FDEs) as follows [26]:

$$\begin{aligned} D^\nu \theta_1(t) &= -\lambda \theta_1(t), & \theta_1(0) &= \theta_1^0, \\ D^\nu \theta_2(t) &= \lambda \theta_1(t) - \mu \theta_2(t), & \theta_2(0) &= \theta_2^0. \end{aligned} \quad (4)$$

The parameters λ and μ denote the rate law constants [25].

The exact solution of this system (4) is presented in the following forms [18]:

$$\begin{aligned}\theta_1(t) &= \theta_1^0 E_\nu(-\lambda t^\nu), \\ \theta_2(t) &= \theta_1^0 \lambda \sum_{\ell_1=0}^{\infty} \sum_{\ell_2=0}^{\infty} \frac{(-\lambda)^{\ell_1} (-\mu)^{\ell_2}}{\Gamma((\ell_1 + \ell_2 + 1)\nu + 1)} t^{(\ell_1 + \ell_2 + 1)\nu}.\end{aligned}\quad (5)$$

3.2 Description of the EV model

The epidemic model of the EVD, in its most general and practical form, is characterized by a set of FDEs. We can express this in the following way [26]:

$$\begin{aligned}D^\nu \psi_1(t) &= -\gamma N - \alpha \psi_1(t) \psi_2(t) + \beta \psi_3(t), & \psi_1(0) &= \hat{\psi}_1^0, \\ D^\nu \psi_2(t) &= \alpha \psi_1(t) \psi_2(t) - (\varepsilon + \delta) \psi_2(t), & \psi_2(0) &= \hat{\psi}_2^0, \\ D^\nu \psi_3(t) &= \delta \psi_2(t) - \beta \psi_3(t), & \psi_3(0) &= \hat{\psi}_3^0, \\ D^\nu \psi_4(t) &= \varepsilon \psi_2(t) + \gamma N, & \psi_4(0) &= \hat{\psi}_4^0, \quad \nu \in (0, 1].\end{aligned}\quad (6)$$

All constants and variables incorporated in this system are presented in [26].

4. Basic concepts on MFEM

Theorem 1. Consider the function $\psi(z)$ with the following case:

$$D^{\ell\nu} \psi(z) \in C[0, a], \quad \ell = 0, 1, \dots, n+1, \quad \nu \in (0, 1].$$

Then the generalized Taylor expansion (GTE) that includes Caputo FD can be given as [27]:

$$\psi(z) = \sum_{i=0}^n \frac{z^{i\nu}}{\Gamma(i\nu + 1)} D^{i\nu} \psi(0^+) + \frac{D^{(n+1)\nu} \psi(\xi)}{\Gamma((n+1)\nu + 1)} z^{(n+1)\nu}, \quad 0 \leq \xi \leq z. \quad (7)$$

Here, we will present the Generalized Euler Method (GEM) [27], through the next steps:

1. Consider a general IVP in $[0, T]$ in its fractional form [27]:

$$D^\nu \Xi(z) = \Phi(z, \Xi(z)), \quad \Xi(0) = \Xi_0, \quad \nu \in (0, 1]. \quad (8)$$

2. Divide $[0, T]$ into n subintervals $[z_i, z_{i+1}]$ with step size $h = T/n$ and points $z_{i+1} = z_i + h$, for $i = 0, 1, 2, \dots, n$.

3. Use the GTE (7) and the continuous functions $D^{\ell\nu}\Xi(z)$, $\ell=0,1,2$ to rewrite $\Xi(z)$ in the following expansion around $z=z_0=0$:

$$\Xi(z) = \Xi(z_0) + \frac{D^{\nu}\Xi(z_0)}{\Gamma(\nu+1)} z^{\nu} + \frac{D^{2\nu}\Xi(c_1)}{\Gamma(2\nu+1)} z^{2\nu}, \quad 0 \leq c_1 \leq T. \quad (9)$$

4. Substitute by $D^{\nu}\Xi(z_0) = \Phi(z_0, \Xi(z_0))$ with $h = z_1 - z_0$ in the expansion (9), to obtain a formula for $\Xi(z_1)$ as follows:

$$\Xi(z_1) = \Xi(z_0) + \Phi(z_0, \Xi(z_0)) \frac{h^{\nu}}{\Gamma(\nu+1)} + D^{2\nu}\Xi(c_1) \frac{h^{2\nu}}{\Gamma(2\nu+1)}.$$

5. We can obtain the following approximation by ignoring the second-order terms (which include $h^{2\nu}$) in the previous formula if we choose $h \ll 1$, and taking $\xi_h^{\nu} = \frac{h^{\nu}}{\Gamma(\nu+1)}$:

$$\Xi(z_1) = \Xi(z_0) + \xi_h^\nu \Phi(z_0, \Xi(z_0)).$$

6. The general form of the GEM can be obtained by repeating the previous process to produce a sequence of approximate solutions $\Xi_j = \Xi(z_j)$ at nodes z_j , $j = 0, 1, 2, \dots$ as follows:

$$\Xi(z_{j+1}) = \Xi(z_j) + \xi_h^\nu \Phi(z_j, \Xi(z_j)), \quad j = 0, 1, 2, \dots, n-1. \quad (10)$$

7. Finally, the general form of the MFEM scheme used to solve the fractional IVP (8) can be obtained by applying the advanced modification in [28] as follows ($j = 0, 1, 2, \dots, n-1$):

$$\Xi(z_{j+1}) = \Xi(z_j) + \xi_h^\nu \Phi(z_j + 0.5\xi_h^\nu, \Xi(z_j) + 0.5\xi_h^\nu \Phi(z_j, \Xi(z_j))). \quad (11)$$

The error analysis of the presented approximation formula (11) can be estimated through the following lemma and theorem.

Lemma 1. [29] Assume that ν and ρ are from \mathbb{R}^+ and $(\lambda_j)_{j=0}^n$ is a sequence satisfying $\lambda_0 \geq \frac{-\rho}{\nu}$ and

$\lambda_{j+1} \leq (1+\nu)\lambda_j + \rho$, $\forall j = 0, 1, 2, \dots, n$. Then we have

$$\lambda_{j+1} \leq e^{(j+1)\nu} \left(\lambda_0 + \frac{\rho}{\nu} \right) - \frac{\rho}{\nu}.$$

Theorem 2. [28] Suppose that the real-valued function Φ is continuous and confirm the Lipschitz criterion:

$$|\Phi(z, \Xi_1) - \Phi(z, \Xi_2)| \leq \kappa |\Xi_1 - \Xi_2|, \quad \kappa > 0.$$

Also, if there is exist a constant ε with $|D^{\nu\chi} \Xi(z)| \leq \varepsilon$, $\forall z \in [a, b]$. Then, we find:

$$|\Xi(z_s) - \Xi_s| \leq \rho(e^{s\chi} - 1), \quad s = 0, 1, 2, \dots, n, \quad (12)$$

where ρ and χ are defined as follows:

$$\rho = \frac{2\Gamma^2(\nu+1)h^{2\nu}\varepsilon}{\Gamma(2\nu+1)(2\Gamma(\nu+1)h^\nu + h^{2\nu}\kappa)}, \quad \chi = \frac{2\Gamma(\nu+1)h^\nu + h^{2\nu}\kappa}{2\Gamma^2(\nu+1)}.$$

5. Numerical implementation

5.1. Numerical implementation to solve fractional BEC model

Here, we are going to obtain approximate solutions for the fractional BEC system by utilizing the MFEM. To achieve this aim, we will rewrite the system (4) as follows:

$$D^\nu \theta_r(t) = g_r(t, \theta_1, \theta_2), \quad r = 1, 2, \quad (13)$$

where the functions g_r , $r = 1, 2$ are given in the system of equations (4). Assuming that the functions $D^{p\nu} \theta_r(t)$, $p = 0, 1, 2$ are continuous on $(0, T]$, let us construct the approximation values of $\theta_r(t_j)$, $r = 1, 2$

for the model (13) utilizing the given approximation form (11) with its iterative formula as follows:

$$\theta_r(t_{j+1}) = \theta_r(t_j) + \xi_h^V g_r(t_j + 0.5\xi_h^V, \theta_r(t_j) + 0.5\xi_h^V g_r(t_j, \theta_1(t_j), \theta_2(t_j))), \quad r=1,2. \quad (14)$$

5.2. Numerical implementation to solve fractional EVD model

Here we will acquire numerical solutions of the EVD model by utilizing the MFEM. To achieve this purpose, we rewrite this model (6) in the following fractional form:

$$D^V \psi_r(t) = g_r(t, \psi_1, \psi_2, \psi_3, \psi_4), \quad r=1,2,3,4, \quad (15)$$

where the functions $g_r, r=1,2,3,4$, are given in the system (6). Assuming that the functions $D^{pV} \psi_r(t)$, $p=0,1,2$ are continuous on $(0,T]$, let us construct the approximation values of $\psi_r(t_j)$, $r=1,2,3,4$ for the model (15) by utilizing the defined approximate scheme (11) with its iterative form as follows:

$$\psi_r(t_{j+1}) = \psi_r(t_j) + \xi_h^V g_r(t_j + 0.5\xi_h^V, \psi_r(t_j) + 0.5\xi_h^V g_r(t_j, \psi_1(t_j), \psi_2(t_j), \psi_3(t_j), \psi_4(t_j))). \quad (16)$$

6. Numerical results

6.1. For the BEC model

We consider the system (4) with distinct values of n, ν at $\mu=0.084457$ and $\lambda=0.018713$ & ICs $\theta_1^0=500$, $\theta_2^0=0$ in $[0,100]$. This is to simulate the BEC numerically by applying the numerical technique in the previous section through Figures 1-3 [30].

1. Figure 1 gives the numerical and exact solutions for $n=240$ at $\nu=0.95$.
2. Figure 2 identifies the absolute true error (ATE) with $n=200$ at $\nu=0.85$.
3. Figure 3 illustrates the impact of the fractional order on the approximate solution at $n=200$ on the same I.Cs.

After carefully looking at these three figures, it's clear that the changing amounts of n, ν have a big effect on how the approximate solution behaves. This shows that the proposed numerical scheme can solve the model (4). Finally, the main conclusion is that the approximate solutions $\theta_k(t)$, $k=1,2$ agree well in their behavior with the real meaning of the problem.

To examine the accuracy of the given technique, different error norms have been computed using the following expressions:

$$L_{\infty} = \max_i |\varphi_i^* - \varphi_i|, \quad L_2 = \sqrt{\left(\sum_{i=1}^n |\varphi_i^* - \varphi_i|^2 \right)}, \quad (17)$$

where, φ_i^* and φ_i represent exact and numerical solutions, respectively.

To check the convergence of the solutions at $(\mu = 0.084457, \lambda = 0.018713, \nu = 0.95)$, we implemented the GEM to solve the system as the benchmarking to the given MFEM in terms of accuracy and efficiency. The following table demonstrates the efficacy of the MFEM in comparison to the benchmark technique in solving the BEC system (4) at diverse values of h and ν . Table 1 evidences that the maximum approximate absolute errors decrease when h decreases. Consequently, the errors demonstrated ample proof of the numerical convergence of the suggested numerical scheme.

6.2 For the EVD model

We consider the system (6) at different values of $n, \nu, \delta, \gamma, \varepsilon, N, \alpha, \beta$ in $[0,5]$. This is to solve numerically the EVD by applying the numerical technique referred to in the previous section. We take the following 2 cases of the I. Cs [31]:

Case 1: $\psi_1^0 = 100, \psi_2^0 = 10, \psi_3^0 = 0, \psi_4^0 = 0;$

Case 2: $\psi_1^0 = 70, \psi_2^0 = 2, \psi_3^0 = 0, \psi_4^0 = 0.$

We conduct a numerical study of the model (6) by implementing the specified strategy as shown in Figures 4-8.

1. Figure 4, displays the approximate solution by the suggested technique & the solution using the RK4M (at $\nu=1$) at $\alpha=0.001, \beta=0.002, \gamma=0.01, \delta=0.004, \varepsilon=0.006, n=40$, and the same I. Cs as in Case 2.
2. Figure 5 shows the numerical solutions found using the suggested method and those found using the technique in [31] at $\nu=0.9$, with the same values for the parameters as shown in Figure 4, and the same I.Cs as in Case 1.
3. Figure 6 illustrates the relative approximate error (RAE) at $\nu=0.95$, with the I. Cs provided by Case 1, and the following values of parameters:
 $\alpha=0.01, \beta=0.02, N=1000, \gamma=0.01, \delta=0.0, \varepsilon=0.6, n=50.$
4. Figure 7 gives how ν (fractional-order) changes the approximate solution for $\nu=0.7, 0.8, 0.9, 1.0$ with the same values for the parameters as shown in Figure 4, and the same I. Cs as in Case 2.

5. Figure 8 estimates how γ changes the approximate solution for $\gamma = 0.005, 0.010, 0.015, 0.020$ using the I. Cs from Case 2 and keeping the same values for the parameters as shown in Figure 6.

After carefully looking at these five figures, it's clear that the changing amounts of $n, \nu, \delta, \gamma, \varepsilon, \alpha, \beta$ have a big effect on how the approximate solution behaves. This shows that the proposed numerical scheme can solve the model (6). Finally, the main observation is that the approximate solutions agree well in their behavior with the real meaning of the problem through different values of those variables contained in the same system. Our results highlight the importance of fractional derivatives in reinforcing model accuracy in capturing complex disease dynamics. These investigations contribute to a deeper understanding of the dynamics of this virus and provide valuable insights for improving disease modeling while providing a solid foundation for predicting outbreaks and planning effective control measures.

Furthermore, to establish the accuracy of our approximate solutions for the system under examination, and show the impact of h , we estimated the infinity error norms in Table 2 with various values of

$h = 0.2, 0.1, 0.05, 0.025$, at $\nu = 0.98$ and $\alpha = 0.001, \beta = 0.002, \gamma = 0.01, \delta = 0.004, \varepsilon = 0.006$.

7. Conclusions

The MFEM was used in this study to get approximate solutions for the Caputo fractional BEC system, and EVD model. This work employed more choices of the fractional order and the included parameters to obtain solutions for the problems under investigation. Moreover, we have ascertained that the given methodology efficiently analyzes these models. Moreover, decreasing the value of h enables us to regulate the precision of the approximate solution. The results we got show that the suggested plan works well at copying the two models, showing both accuracy and computer efficiency. In the future, we will attempt to study the convergence and stability of the method proposed here in greater depth, in addition to making any further modifications to the technique to increase the efficiency and accuracy of solutions. Finally, we will address the same process with other types of fractional derivatives.

Acknowledgements

This work was supported and funded by the Deanship of Scientific Research at Imam Mohammad Ibn Saud Islamic University (IMSIU) (grant number IMSIU-DDRSP2503).

References

1. Amundsen, S.B. "Historical analysis of the Ebola virus: Prospective implications for primary care nursing today", *The Journal for Nurse Practitioners*, **2**, pp. 343-351 (1998). [https://www.semanticscholar.org/paper/Historical-analysis-of-the-Ebola-virus/\\$3A-prospective-b/6eb7d7b41199698445308ee237887124da4d8ad6](https://www.semanticscholar.org/paper/Historical-analysis-of-the-Ebola-virus/$3A-prospective-b/6eb7d7b41199698445308ee237887124da4d8ad6)
2. Area, I., Batarfi, H. Losada, J., et al. "On a fractional order Ebola epidemic model", *Advances in Difference Equations*, **2015**, pp. 1-8 (2015). <https://advancesincontinuousanddiscretemodels.springeropen.com/articles/10.1186/>

3. Mazandu, G.K. Nembaware, V., Thomford, N.E. et al. "A potential roadmap to overcome the current eastern DRC Ebola virus disease outbreak: From a computational perspective", *Scientific African*, **7**, pp. 1-10 (2020).
<https://doi.org/10.1016/j.sciaf.2020.e00282>
4. Zanib, S.A. Ramzan, S., Abbas, N., et al. "Comprehensive analysis of a conformable mathematical model of Ebola virus with effective control strategies", *Scientia Iranica*, **13**, pp. 15-25 (2024). <https://scientiairanica.sharif.edu/article-23693>.
5. Zanib, S.A., Ramzan, S. Shah, M.A., et al. "Comprehensive analysis of the mathematical model of HIV/AIDS incorporating Fisher-Folk community" *Modeling Earth Systems and Environment*, **10**, pp. 6323–6340 (2024).
<https://link.springer.com/article/10.1007/s40808-024-02099-9>
6. Ramzan, S., Zanib, S.A., Shah, M.A., et al. "Analytical study of a modified monkeypox virus model using Caputo-Fabrizio fractional derivatives", *Modeling Earth Systems and Environment*, **10**, pp. 6475-6492 (2024).
<https://link.springer.com/article/10.1007/s40808-024-02115-y>
7. Nisar, K.S., Farman, M., Jamil, K., et al. "Computational and stability analysis of Ebola virus epidemic model with piecewise hybrid fractional operator", *PLOS ONE*, **19**(4), pp. 1-43 (2024). <https://doi.org/10.1371/journal.pone.0298620>
8. Naik, P.A., Farman, M., Jamil, K., et al. "Modeling and analysis using the piecewise hybrid fractional operator in time scale measure for Ebola virus epidemics under Mittag-Leffler kernel", *Scientific Reports*, **14**(24963), pp. 1-23 (2024).
<https://doi.org/10.1038/s41598-024-75644-2>
9. Nisar, K.S., Shoaib, M., Raja, M.A.Z., et al. "A novel design of evolutionary computing to study the quarantine effects on transmission model of Ebola virus disease", *Results in Physics*, **48**, pp. 1-16 (2023). <https://doi.org/10.1016/j.rinp.2023.106408>
10. Yadav, P., Jahan, S., Nisar, K.S. "Fractional order mathematical model of Ebola virus under Atangana-Baleanu-Caputo operator", *Results in Control and Optimization*, **13**, pp. 1-15 (2023). <https://doi.org/10.1016/j.rico.2023.100332>
11. Nazir, A., Ahmed, N., Khan, U. "An advanced version of a conformable mathematical model of Ebola virus disease in Africa", *Alexandria Engineering Journal*, **59**(5), pp. 3261-3268 (2020). <https://doi.org/10.1016/j.aej.2020.08.050>

12. Bonyah, E., Badu, K., and Asiedu-Addo, S.K. "Optimal control application to an Ebola model", *Asian Pacific Journal of Tropical Biomedicine*, **6**, pp. 283-289 (2016).
<https://doi.org/10.1016/j.apjtb.2016.01.012>
13. Koca, I. "Modelling the spread of Ebola virus with Atangana-Baleanu fractional operators", *European Physical Journal - Plus*, **133**(3), pp. 100-110 (2018).
<https://link.springer.com/article/10.1140/epjp/i2018-11949-4>
14. Rachah, A. and Torres, D.F.M. "Predicting and controlling the Ebola infection", *Mathematical Methods in the Applied Sciences*, **40**, pp. 6155-6164 (2017).
<https://doi.org/10.1002/mma.3841>
15. Gejji, V.D., Sukale Y., and Bhalekar, S. "A new predictor-corrector method for fractional differential equations", *Applied Mathematics and Computation*, **244**, pp. 158-182 (2014). <https://doi.org/10.1016/j.amc.2014.06.097>
16. Green, C.W.H., and Yan, Y. "Detailed error analysis for a fractional Adams Method on Caputo- Hadamard fractional differential equations", *Foundations*, **2**(4), pp. 839-861 (2022). <https://doi.org/10.3390/foundations2040057>
17. Ludwin, C. "Blood alcohol content", *Undergraduate Journal of Mathematical Modeling*, **3**(2) pp. 1-15 (2011). <http://dx.doi.org/10.5038/2326-3652.3.2.1>
18. Qureshi, S., Yusuf, A., Shaikh, A.A., et al. "Fractional modeling of blood ethanol concentration system with real data application", *Chaos*, **29**, 013143 (2019).
<https://doi.org/10.1063/1.5082907>
19. Zanib, S.A., Zubair, T., Abbas, N., et al. "An advanced ABC finite difference approach for modified mathematical modeling of alcohol consumption dynamics", *Modeling Earth Systems and Environment*, **11**(130), pp. 1-15 (2025).
<https://link.springer.com/article/10.1007/s40808-025-02307-0>
20. Ramzan, S., Zanib, S.A., Shah, M.A., et al. "On bifurcation analysis and numerical investigation of alcohol consumption dynamics", *Modern Physics Letters B*, **39**(18), 2550040 (2025). <https://doi.org/10.1142/S021798492550040X>
21. Kilbas, A.A., Srivastava, H.M., and Trujillo, J.J. "*Theory and Applications of Fractional Differential Equations*", Vol. 204, Elsevier (North-Holland) Science Publishers, Amsterdam, London and New York (2006).
22. Adel, M., Srivastava, H.M., and Khader, M.M. "Implementation of an accurate method for the analysis and simulation of electrical R-L circuits", *Mathematical Methods in the Applied Sciences*, **46**, pp. 8362-8371 (2023).

23. Shloof, A.M., Senu, N., Ahmadian, A., et al. "Solving fractal-fractional differential equations using an operational matrix of derivatives via Hilfer fractal-fractional derivative sense", *Applied Numerical Mathematics*, **178**, pp. 1-29 (2022).
<https://doi.org/10.1016/j.apnum.2022.02.006>
24. Aboubakr, A.F.S., Ismail, G.M., Khader, M.M. "Derivation of an approximate formula of the Rabotnov fractional-exponential kernel fractional derivative and applied it for numerically solving the blood ethanol concentration systems", *AIMS Mathematics*, **8**(12), pp. 30704-30716 (2023).
<https://www.aimspress.com/article/doi/10.3934/math.20231569>
25. Ludwin, C. "Blood alcohol content", *Journal of Mathematical Modeling*, **3**(2), pp. 1-10 (2011). <http://dx.doi.org/10.5038/2326-3652.3.2.1>
26. Khader, M.M., and Babatin, M.M. "Designing an efficient numerical method for solving the Blood Ethanol Concentration system and Ebola Virus Models", *European Journal of Pure and Applied Mathematics*, **17**(4), pp. 3167-3184 (2024).
<https://doi.org/10.29020/nybg.ejpam.v17i4.5447>
27. Zaid, M.O. and Shawagfeh, N.T. "Generalized Taylor's formula", *Applied Mathematics Computation*, **186**, pp. 286-293 (2007). <https://doi.org/10.1016/j.amc.2006.07.102>
28. I.M. Batiha, A. Bataihah, Abeer A. Al-Nana, et al. "A numerical scheme for dealing with fractional initial value problem", *International Journal of Innovative Computing, Information and Control*, **19**, pp. 763-774 (2023). <https://doi.org/10.24507/ijicic.19.03.763>
29. Burden, R.L., and Faires, J.D. *Numerical Analysis*, 9th Edition, Brookscole, Boston, (2011).
30. Khader, M.M., and Saad, K.M. "Numerical treatment for studying the blood ethanol concentration systems with different forms of fractional derivatives", *International Journal of Modern Physics C*, **31**(3), 2050044 (2020).
<https://doi.org/10.1142/S0129183120500448>
31. Srivastava, H.M., Saad, K.M., and Khader, M.M. "An efficient spectral collocation method for the dynamic simulation of the fractional epidemiological model of the Ebola virus", *Chaos, Solitons & Fractals*, **140**, pp. 1-7 (2020).
<https://doi.org/10.1016/j.chaos.2020.110174>

Biographies

Mohamed M. Khader obtained his PhD in Numerical Analysis from Benha University, Benha, Egypt. Currently, he is a Professor at Mathematics Department, Benha University (Egypt) and Imam Mohammad Ibn Saud Islamic University (KSA). His main research areas are: Numerical Analysis and Mathematical Physics, Including Numerical Methods for Nonlinear Differential Equations. He has published research articles in reputed international journals of mathematical and engineering sciences.

Aml M. Shloof received her PhD in Numerical Analysis from University of Zintan, AlZintan, Libya. Currently, she is a Lecture at Mathematics Department, University of Zintan. Her main research areas are: Numerical Analysis and Mathematical Physics, Including Numerical Methods for Nonlinear Differential Equations.

Halema Ali Hamead received her PhD in Numerical Analysis from University of Aljufra, Aljufra, Libya. Currently, she is a Lecture at Mathematics Department, University of Aljufra. Her main research areas are: Numerical Analysis and Mathematical Physics, Including Numerical Methods for Nonlinear Differential Equations.

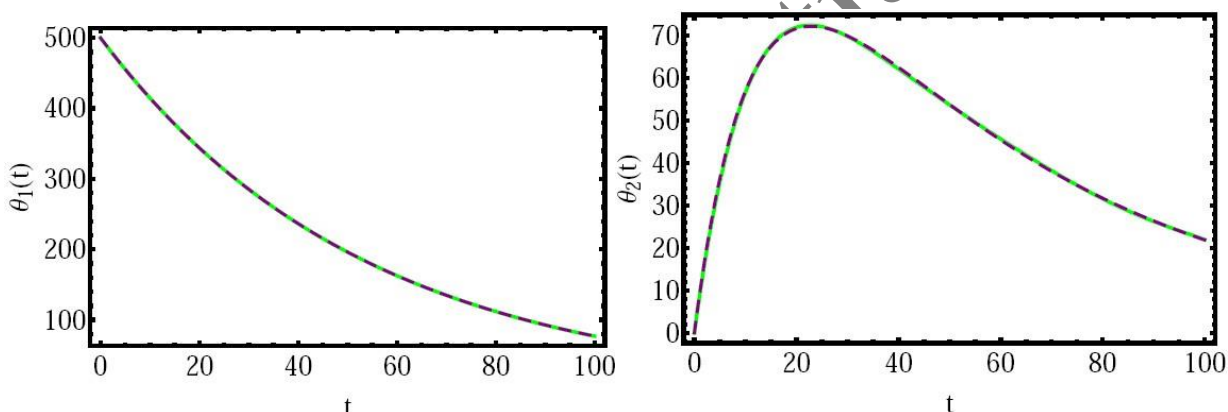


Figure 1. The numerical and exact solutions at $n = 240$, $\nu = 0.95$.

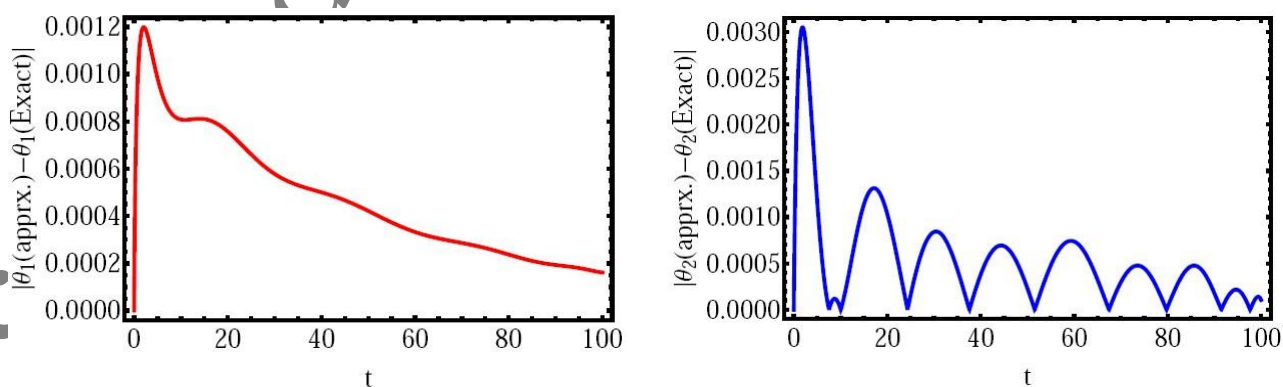


Figure 2. The ATE at $n = 200$ and $\nu = 0.85$.

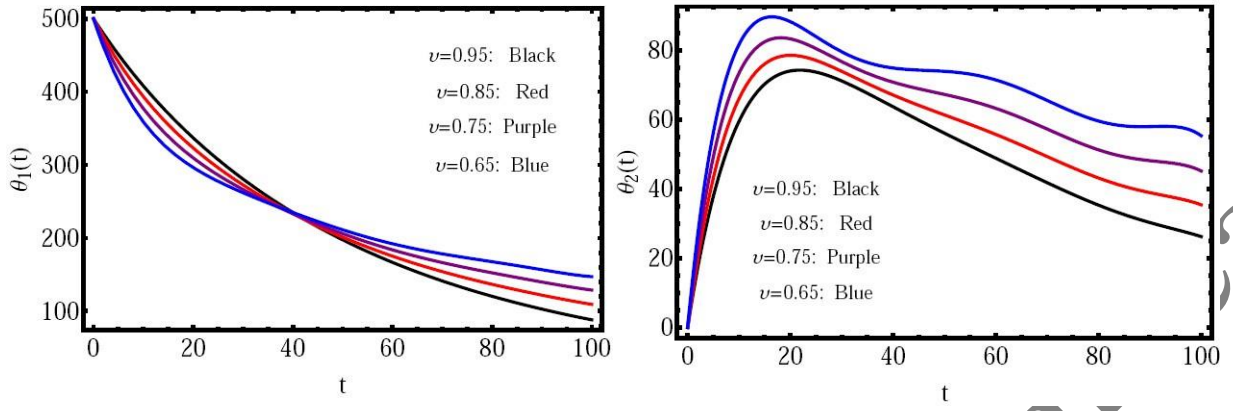


Figure 3. The numerical solution at $n = 200$ with distinct fractional-order ν .

Table 1. A comparison of the highest estimated absolute errors in solving the BEC model (4) at various values of ν, h .

Method	ν/h	$h=1$	$h=1/2$	$h=1/4$	$h=1/8$	$h=1/16$
MFEM	0.75	0.1478E-3	7.2510E-4	4.5008E-5	7.2984E-6	2.2587E-7
GEM		8.0215E-2	5.0147E-3	6.0287E-4	2.1239E-5	4.0589E-5
MFEM	0.85	7.2584E-3	8.2501E-4	5.0841E-5	5.2419E-6	5.0490E-7
GEM		6.0258E-2	2.1187E-3	0.0147E-4	8.0014E-5	1.9527E-6
MFEM	0.95	1.2587E-4	4.0258E-4	2.2879E-5	8.2510E-6	7.2901E-7
GEM		0.0147E-3	6.7165E-3	3.3402E-4	7.2581E-5	8.3687E-5

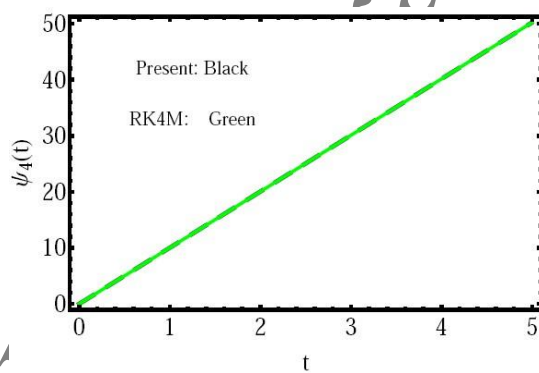
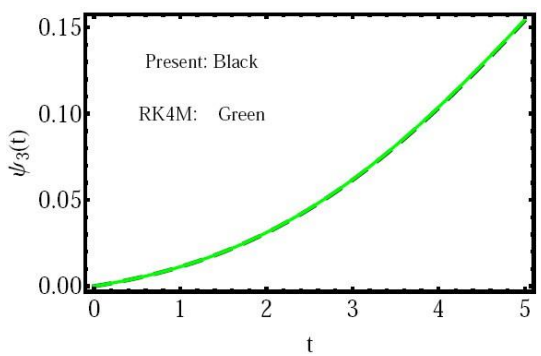
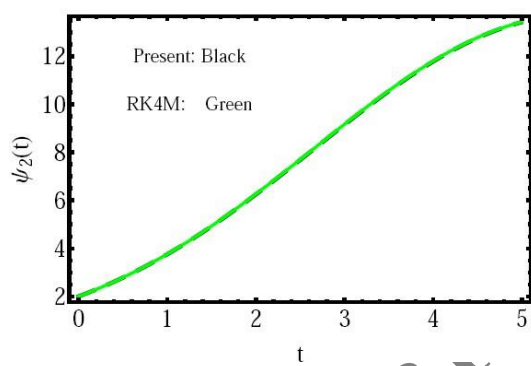
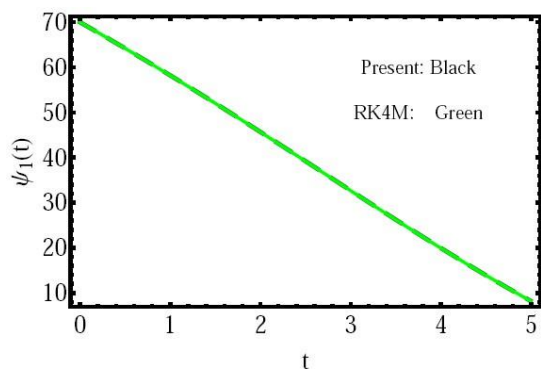


Figure 4. The approximate solutions & the solution by RK4M with the Case 2 of the I.Cs.

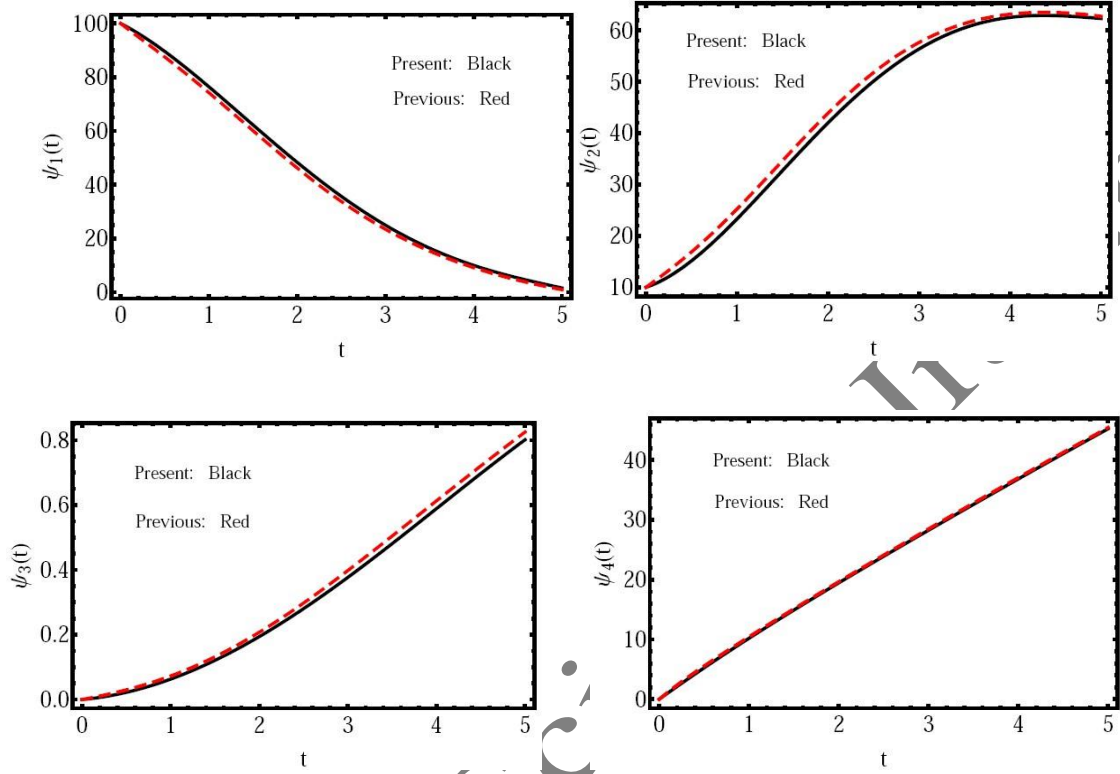


Figure 5. The current solution & approximate solution [31] at the Case 1 of the I.Cs.

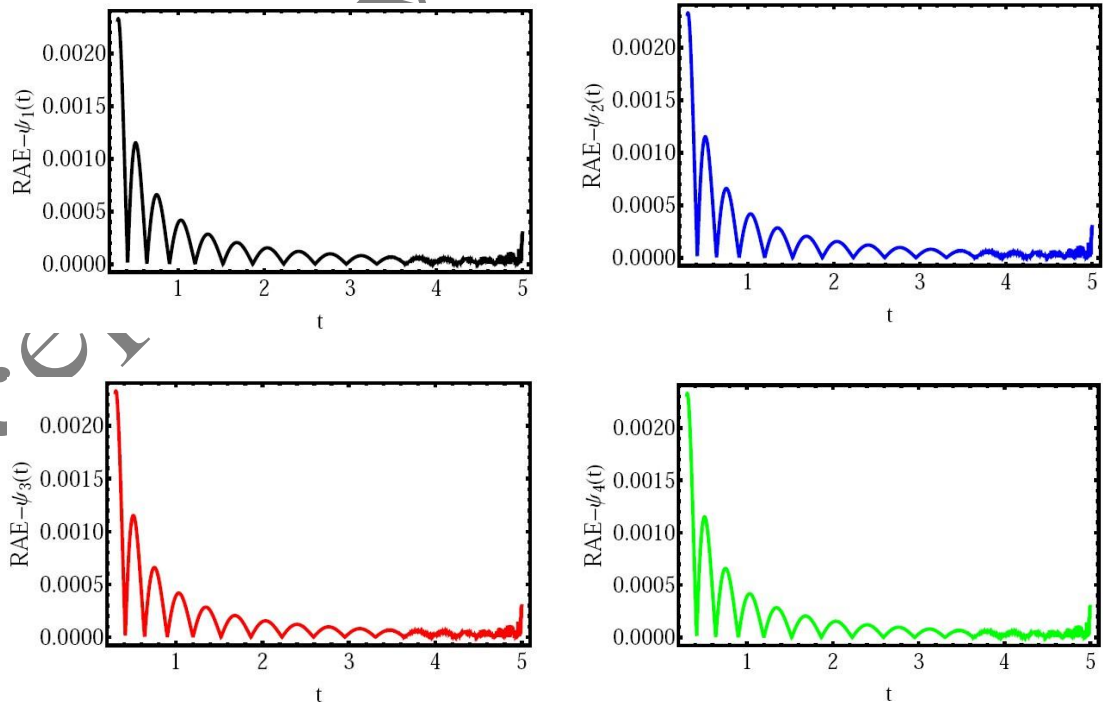


Figure 6. The RAE at $\nu = 0.95$ with the Case 1 of the I.Cs.

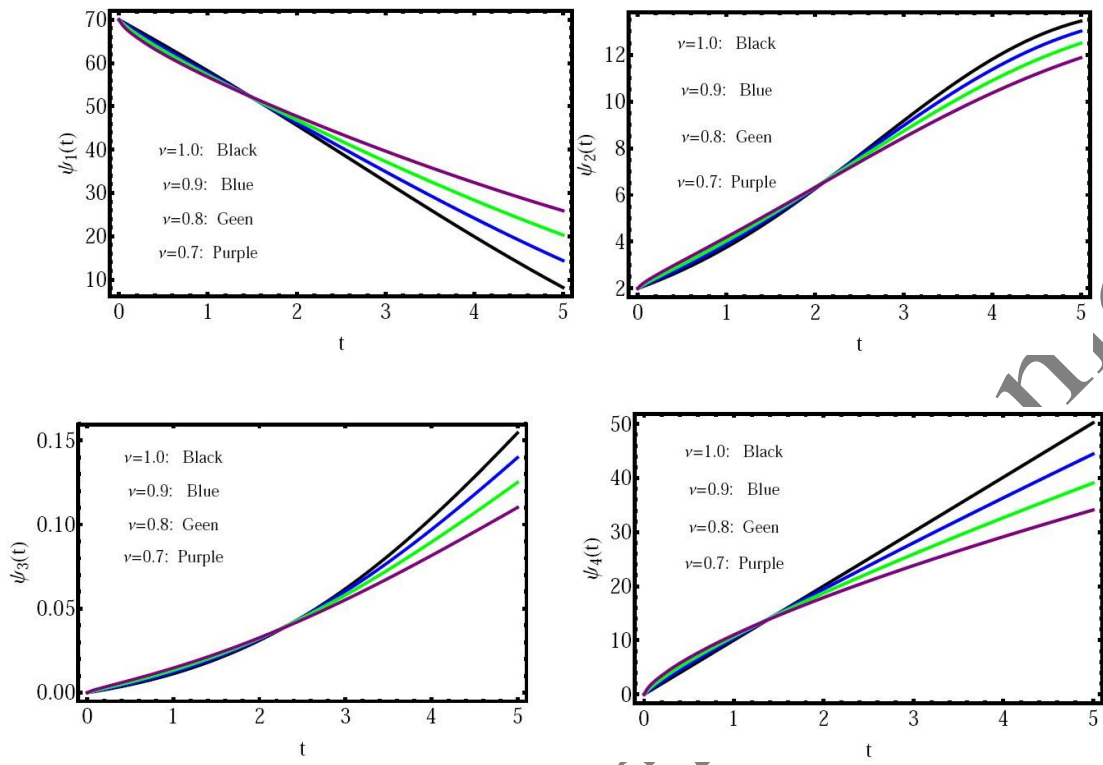


Figure 7. The influence of ν on the approximate solution with the Case 2 of the I.Cs.

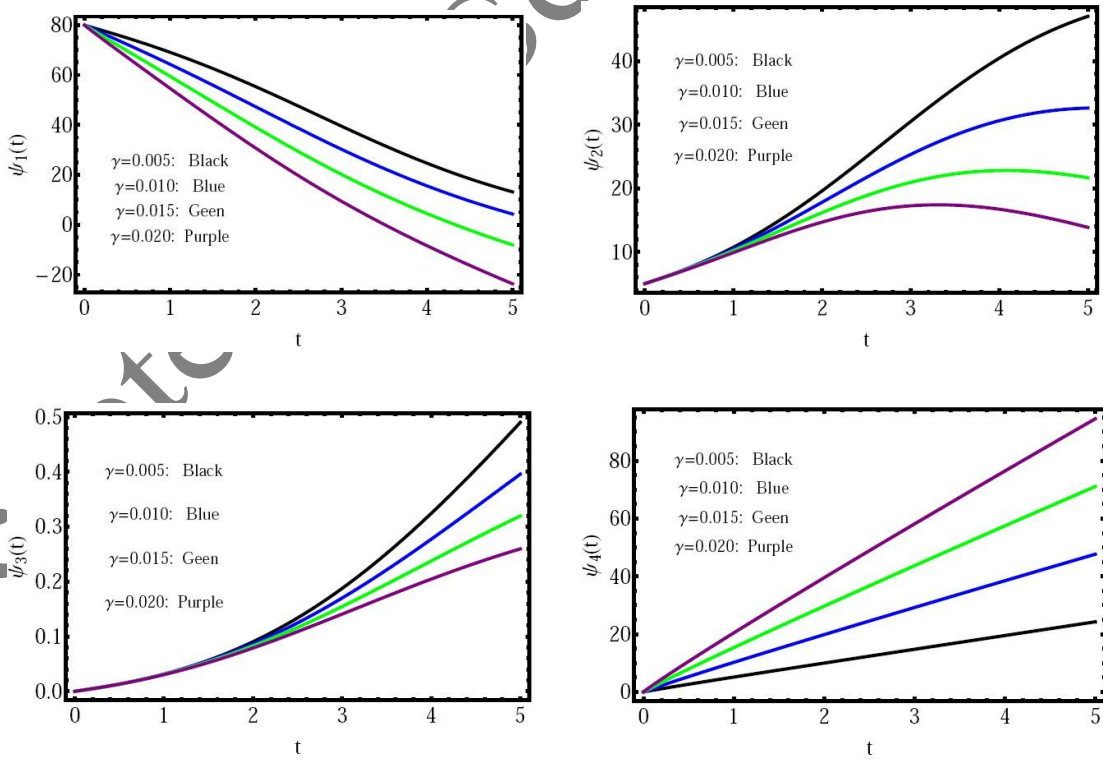


Figure 8. The influence of γ on the approximate solution with the Case 2 of the I.Cs.

Table 2. The infinity error norms of $\psi_r(t)$, $r = 1, 2, 3, 4$ in the model (6) with various values of h and Case 2 of I.Cs.

h	$L_\infty - \psi_1$	$L_\infty - \psi_2$	$L_\infty - \psi_3$	$L_\infty - \psi_4$
0.20	6.2874E-04	6.0287E-04	4.0147E-05	2.2104E-05
0.10	0.2547E-05	4.0258E-05	5.0147E-06	7.2081E-06
0.05	5.0214E-06	5.2141E-06	4.2017E-07	6.3309E-07
0.025	0.2179E-07	7.2301E-07	9.0014E-08	2.2597E-08

Accepted by Scientia Iranica